The Role of Photophysics Processes in Thermal Lens Spectroscopy of Fluids: A Theoretical Study.

ARTICLE *in* THE JOURNAL OF PHYSICAL CHEMISTRY A · JULY 2014

Impact Factor: 2.69 · DOI: 10.1021/jp505255a · Source: PubMed

5 AUTHORS, INCLUDING:

Luis Carlos Malacarne
Universidade Estadual de Maringá
102 PUBLICATIONS **1,013** CITATIONS
SEE PROFILE

Mauro Luciano Baesso
Universidade Estadual de Maringá
318 PUBLICATIONS **3,429** CITATIONS
SEE PROFILE

Ervin Lenzi
State University of Ponta Grossa
190 PUBLICATIONS **1,826** CITATIONS
SEE PROFILE

Nelson G. C. Astrath
Universidade Estadual de Maringá
110 PUBLICATIONS **754** CITATIONS
SEE PROFILE

Discriminating the role of sample length in thermal lensing of solids

T. P. Rodrigues,[1] V. S. Zanuto,[1] R. A. Cruz,[2,3] T. Catunda,[2] M. L. Baesso,[1] N. G. C. Astrath,[1,4] and L. C. Malacarne[1,5]

[1]Departamento de Física, Universidade Estadual de Maringá, Maringá, PR 87020-900, Brazil

[2]Instituto de Física de São Carlos, Universidade de São Paulo, São Carlos, SP 13560-970, Brazil

[3]Currently at Instituto Federal de Educação, Ciência e Tecnologia de São Paulo—Campus Avaré, Avaré, SP 18708-150, Brazil

[4]e-mail: astrathngc@pq.cnpq.br

[5]e-mail: lcmala@pq.cnpq.br

Received March 31, 2014; revised April 29, 2014; accepted May 25, 2014;
posted May 27, 2014 (Doc. ID 209164); published June 30, 2014

Thermal lens (TL) is a key effect in laser engineering and photothermal spectroscopy. The amplitude of the TL signal or its dioptric power is proportional to the optical path difference (OPD) between the center and border of the beam, which is proportional to the heat power (Ph). Due to thermally induced mechanical stress and bulging of end faces of the sample, OPD depends critically on the geometry of the sample. In this investigation, TL measurements were performed as a function of the sample length keeping the same Ph. It is experimentally demonstrated that for materials with positive $\partial n/\partial T$ OPD increases typically 30 to 50% with the decrease of sample length (from long rod to thin-disk geometry). For materials with negative $\partial n/\partial T$, this variation is much larger due to the cancelation of the different contributions to OPD with opposite signs. Furthermore, the experimental investigation presented here validates a recently proposed unified theoretical description of the TL effect.

OCIS codes: (300.6430) Spectroscopy, photothermal; (350.5340) Photothermal effects.
http://dx.doi.org/10.1364/OL.39.004013

The description of wavefront distortion induced by laser absorption in optical elements is fundamental in the design and evaluation of solid state lasers, optical windows, and other passive optical components for high power laser systems [1–5]. Thermal lensing is the dominant effect for beam quality and power scaling of solid state lasers. The calculation and experimental determination of the dioptric power of the thermal lens (TL) effect is very important in several applications. Much effort has been made on the study of diode pumped solid state lasers (DPSSL), especially when operating in an end-pumping configuration due to the highly localized heat deposition achieved in this configuration [1]. For instance, compensation of TL effects is a key issue for the performance of interferometric gravitational-wave detectors [2]. Monitoring the dynamic process of optical path difference (OPD) with photothermal methods enables direct quantitative access to many physical properties of a large class of materials. In general, pump-probe photothermal techniques are attractive as highly sensitive, fast, noncontacting, and nondestructive methodologies [6].

In liquids the TL effect is governed by the temperature coefficient of the refractive index, $\partial n/\partial T$. However, for solids the problem is more complex because the OPD is strongly affected by thermal expansion that leads to elongation and bulging of the end faces in addition to the mechanical stress. The relative magnitude of these three different contributions to OPD depends critically on the geometry of the sample and its physical properties. Sometimes, the TL effect is diminished due to the negative sign of these terms, usually $\partial n/\partial T$ [7]. Analytical expressions for OPD calculation, and consequently the effective value of TL focal length, f_{th}, or dioptric power, $\mathcal{D}_{\mathrm{th}}$ ($f_{\mathrm{th}} = \mathcal{D}_{\mathrm{th}}^{-1}$), are available only in the limiting cases of the so called "thin-disk" or "long-rod" using the plane-stress and plane-strain approximations, respectively [4,5]. Consequently, numerical methods (mostly finite element analysis) are required for an in-depth analysis of many problems. Recently, Malacarne and co-workers [8,9] obtained an analytical expression for OPD calculation for samples with arbitrary thickness. This proposed "unified theoretical model" is an important step toward the understanding of OPD in optical materials, according to an OSA Spotlight comment [10].

The dual-beam mode-mismatched thermal lens (MMTL) spectrometry was developed to improve the sensitivity of TL measurements. It is a very sensitive, accurate, and simple method for the determination of TL induced phase-shifts and thermo-optical properties of laser materials, such as thermal diffusivity and the fluorescence quantum efficiency (η) of laser media, without requiring complicated setups or calibration procedures [11]. This method was used to determine the temperature coefficient of the optical path of several laser and optical materials [12]. It was also applied to determine f_{th} and the thermal load of a diode end-pumped Nd:YAG laser (oscillating at 1.06 and 1.34 μm) [13]. In this study, the MMTL method was used to determine the evolution of the f_{th} with the sample length in order to discriminate the effect of thermal stress. The experiments were performed in four different materials: calcium aluminosilicate (CAS), Q98 from Kigre Inc., and BK7 borosilicate and Zerodur glass from Schott. These materials were selected for their thermo-optical properties (Table 1). CAS is typical oxide glass with positive $\partial n/\partial T$ and positive linear thermal expansion coefficient [14,15]. Q98 is a Nd^{3+} doped phosphate glass with negative $\partial n/\partial T$, which was designed to be an athermal optical material. BK7 is a typical highly transparent borosilicate glass. Zerodur is a glass ceramic with an extremely low coefficient of thermal expansion. It was observed that the TL signals, and consequently f_{th}, are in complete agreement with the theoretical predictions of the recently developed theory [8,9]. Although, the results reach the expected "thin-disk"

Table 1. Physical Properties of the Samples [14,15]. Parameters for Q98, Zerodur, and BK7 are from Vendors.

Parameter	Units	CAS	Q98	Zerodur	BK7
ρ	kgm^{-3}	2890	3099	2530	2510
n		1.63	1.555	1.54	1.517
c	$Jkg^{-1}\,K^{-1}$	810	800	800	858
k	$Wm^{-1}\,K^{-1}$	1.35	0.82	1.46	1.114
$\partial n/\partial T$	$10^{-6}\ K^{-1}$	5.3	−4.5	14.3	2.5
α_T	$10^{-6}\ K^{-1}$	7.5	9.9	0.02	7.1
A_e	m^{-1}	62	46	18	0.2
ν		0.23	0.24	0.24	0.208
E	10^9 Pa	90	72.1	90.3	81
$q_\parallel$	$10^{-12}\ Pa^{-1}$	0.09	0.35		0.28
$q_\perp$	$10^{-12}\ Pa^{-1}$	0.90	1.95		1.86

and "long-rod" values in their respective limits, we found that the thin-disk formula has been used indiscriminately in the literature, sometimes in situations better described by the long-rod case.

The experiments were performed in a mode-mismatched configuration, as shown in Fig. 1, at room temperature. A continuous wave (cw) TEM_{00} Gaussian excitation laser beam at the wavelength $\lambda_e = 514.5$ nm irradiates a weakly absorbing sample of thickness l_0, inducing a time- dependent temperature gradient and a correspondent thermoelastic surface displacement. A weak TEM_{00} Gaussian beam at $\lambda_p = 632.8$ nm, almost collinearly arranged with the excitation laser beam, travels through the sample and probes the TL. The radii of the excitation and probe beams in the sample are $w_{0e} = 55$ μm and $w_{1p} = 377$ μm, respectively. The confocal distance of the excitation laser beam is $Z_{CE} = 18.5$ mm. The probe beam propagates in the z-direction, and the sample is placed at $z = 0$. The distance between the sample and the probe beam waist of radius ω_{0p} is $Z_1 = 13.3$ cm, and the distance between the sample and the detector plane is $Z_2 = 276.6$ cm. As in most TL analytical approaches, it is assumed that the radial dimensions of the sample are large compared with the excitation beam radius, and the excitation time is short enough to avoid edge effects, i.e., the sample is assumed to be radially infinite.

Figure 2 displays the time-resolved TL transients obtained from the experiments for Zerodur and CAS samples with different thicknesses. For both materials the experiments were designed to compare the TL signal

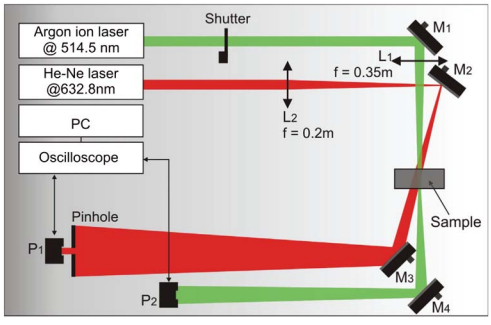

Fig. 1. Schematic diagram of an apparatus for time-resolved TL experiment. L_i, M_i, P_i and f stand for lenses, mirrors, photodiodes, and focal distances, respectively.

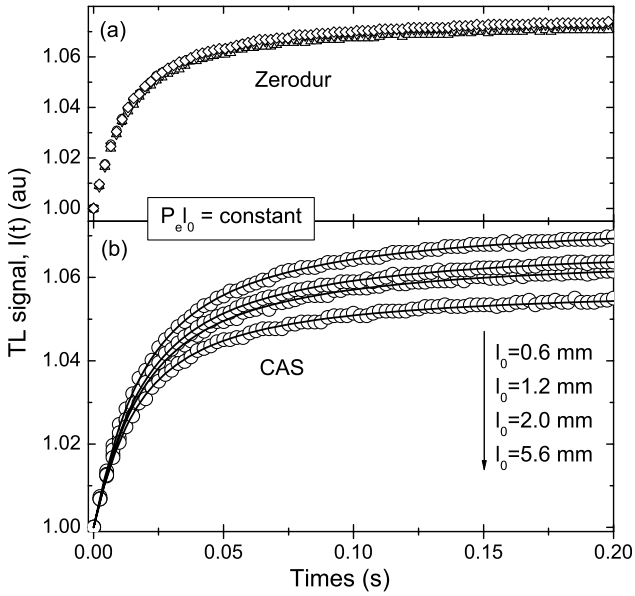

Fig. 2. Experimental TL transients for (a) Zerodur ($l_0 = 0.5, 1.0, 1.9, 3.0, 5.0$ mm) and (b) CAS glasses with the product $P_e l_0$ constant. Open symbols: experimental data; solid lines: best curve fitting.

of the different samples keeping the product $P_e l_0$ constant (P_e is the excitation beam power). The signals from five different Zerodur samples cannot be distinguished while for CAS the signal amplitude increases as the sample thickness is decreased. The Zerodur data can be interpreted by the standard TL theory [11], where the transient signal amplitude is proportional to θ_T,

$$\theta_T = \vartheta l_0 \chi, \tag{1}$$

where $\vartheta = P_e A_e \phi/(k\lambda_p)$. A_e is the optical absorption coefficient at the excitation beam wavelength, k is the thermal conductivity, ϕ is the fraction of absorbed energy converted into heat, and χ is thermo-optical coefficient. The characteristic TL signal response time is given by $t_c = w_{0e}^2/4D$, where $D = k/(\rho c)$ is the thermal diffusivity, in which ρ is the mass density and c is the specific heat. The parameters θ_T and t_c were obtained by fitting the experimental transient signals of Fig. 2 to the standard model [11]. For Zerodur, from t_c the thermal diffusivity value was obtained as $D = (8.2 \pm 0.3) \times 10^{-7}\ m^2/s$, which is in good agreement with the literature (Table 1). Zerodur has no fluorescence under excitation at 514.5 nm, and it can be assumed that all absorbed energy is transformed into heat, i.e., $\phi = 1$. Therefore, using θ_T from regression in Eq. 1, we obtained for Zerodur, as in a liquid, that $\chi \approx \partial n/\partial T$ since this material was designed to have negligible thermal expansion ($\alpha_T \approx 0$). When the factor $P_e l_0$ is constant, the absorbed power is constant and, by Eq. (1), θ_T and the TL signal are also expected to remain the same. Hence, Fig. 2(b) demonstrates that the CAS signal cannot be explained by the standard simplified model. This is clearly shown by the fact that the amplitude of the TL signal decreases as l_0 increases. The problem here is the assumption that the phase profile is proportional to the temperature profile by $\Phi(r,t) \propto \chi T(r,t)$. In fact, due to the thermoelastic effect

in solid samples, this assumption is only valid in two limiting cases: thin disk and long rod. For thin samples, the so-called plane-stress approximation results in [5]

$$\chi^0 = \frac{\partial n}{\partial T} + (n-1)(1+\nu)\alpha_T + \frac{n^3 E \alpha_T}{4}(q_\parallel + q_\perp), \quad (2)$$

where ν is the Poisson's ratio, n is the refractive index of the sample, E is the Young's modulus, and $q_\parallel$ and $q_\perp$ refer to the piezo-optic coefficients for stresses applied parallel and perpendicular to the polarization axis, respectively. The other limit, where the sample thickness is larger than the radius of the region affected by the thermoelastic effect, the so-called "long rod" approach, uses the plane strain approximation [5],

$$\chi^\infty = \frac{\partial n}{\partial T} + \frac{n^3 E \alpha_T}{4(1-\nu)}(q_\parallel + 3q_\perp). \quad (3)$$

Using the published data for CAS we estimate $\chi^0 = 11.8 \times 10^{-6}$ K^{-1} and $\chi^\infty = 7.9 \times 10^{-6}$ K^{-1}. In fact, if we use the simplified theory to fit the experimental data, we obtain $\chi^0 = (11.5 \pm 0.9) \times 10^{-6}$ K^{-1} for the sample with $l_0 = 0.6$ mm and $\chi^\infty = (8.5 \pm 0.8) \times 10^{-6}$ K^{-1} for $l_0 = 5.6$ mm.

In general, samples with arbitrary thickness, can be analyzed using the analytical model recently developed by Malacarne and co-workers [8,9]. In [16] it was shown that the difference introduced in the phase shift by the air-glass heat coupling need only be considered in the case of extremely thin samples. Under normal experimental conditions, the adiabatic second-kind (Neumann) boundary condition at the outer surfaces could be considered. Using the unified model for calculating the laser-induced wavefront distortion in optical materials [8,9], the sample contribution for the phase shift in the case of a moderate optical absorbing material, probed by an axially symmetric unpolarized Gaussian beam, is

$$\Phi(g,t) = \vartheta \int_0^\infty l_0\left(1 - \frac{A_e l_0}{2}\right)\chi(\alpha, l_0) e^{-\frac{1}{8}w_{0e}^2\alpha^2} \times (1 - e^{-\frac{1}{4}w_{0e}^2\alpha^2 t/t_c})\left[J_0\left(\alpha w_{0e}\sqrt{mg}\right) - 1\right]\alpha^{-1}\mathrm{d}\alpha \quad (4)$$

with $m = (w_{1p}/w_{0e})^2$, and

$$\chi(\alpha, l_0) = \frac{\partial n}{\partial T} + \frac{4(n-1)(1+\nu)\alpha_T h(\alpha, l_0)}{l_0\alpha} + \frac{n^3 E \alpha_T}{4(1-\nu)}\left[(q_\parallel + 3q_\perp) - \frac{4[q_\parallel \nu + q_\perp(2+\nu)]h(\alpha, l_0)}{l_0\alpha}\right], \quad (5)$$

where $h(\alpha, l_0) = [\cosh(l_0\alpha) - 1]/[l_0\alpha + \sinh(l_0\alpha)]$. $J_n(x)$ is the Bessel function of the first kind. The factor $[1 - (A_e l_0)/2]$ in Eq. 4 accounts for the effect of moderated optical absorption coefficients. When the sample thickness is smaller than the radius of the region affected by the thermoelastic effect, the above expression reduces to the plane-stress approximation given by Eq. (2), which is indiscriminately used in the literature. In the other limit, for sample thicknesses larger than the radius of the region affected by the thermoelastic effect, Eq. (5) recovers the plane-strain approximation, Eq. (3). We remind the reader that the plane-stress and plane-strain approximations are valid only under the above restrictive conditions.

The thermal characteristic time t_c and the parameter ϑ were obtained from regression using the Fresnel–Kirchhoff diffraction integral

$$I(t) = \frac{|\int_0^\infty \exp[-(1+iV)g - i\Phi(g,t)]\mathrm{d}g|^2}{|\int_0^\infty \exp[-(1+iV)g]\mathrm{d}g|^2} \quad (6)$$

with Eqs. (2), (3), or (5) in the phase shift. $V = Z_1/Z_c + Z_c[1 + (Z_1/Z_c)^2]/Z_2$, $Z_c = 4.65$ cm is the confocal distance of the probe beam. Regressions with the models were performed using the "NonlinearModelFit" function in *Wolfram Mathematica 7*. Using the unified model, it was observed that ϑ presented a linear dependence with P_e, as expected.

Figure 3 presents the parameter ϑ obtained from the fitted TL transients with the unified and approximated theories normalized by the excitation beam power. It shows that the unified model gives the same ϑ/P_e value regardless of the thickness of l_0 for both samples CAS and Q98. It should be noticed that the unified model recovers the limiting cases, thin disk and long rod, in their respective approaches with $\vartheta = \theta_T/(\chi l_0)$. For instance, the "long rod" result is close to the expected value for l_0 larger than 5.5 mm and the "thin disk" for l_0 thinner than 0.5 mm. Similar behavior was observed for $l_0 > 9$ mm and $l_0 < 0.5$ mm in the case of Q98. Moreover, as an athermal glass, Q98 presents negative $\partial n/\partial T$ that cancels the

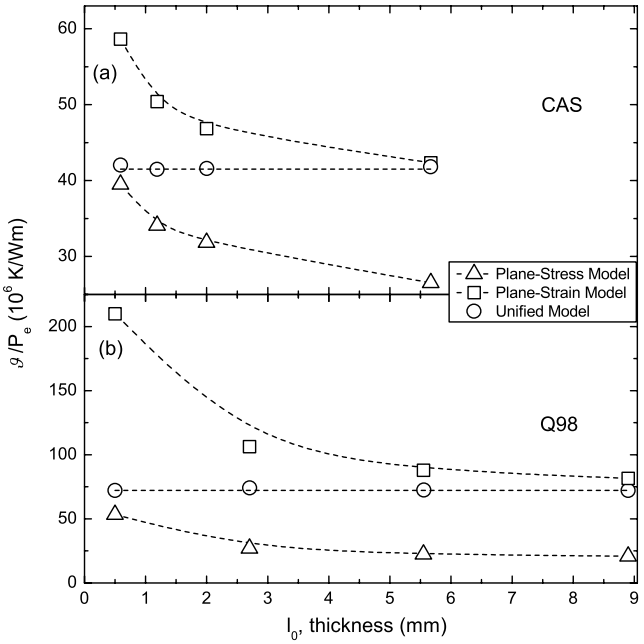

Fig. 3. Parameter ϑ/P_e versus l_0 obtained by the fit of experimental data for (a) CAS and (b) Q98 glasses using the models: (open circle) unified model, (open square) plane-stress approximation, and (open triangle) plane-strain approximation. Dashed lines are guides for the eye. The standard deviations are smaller than 5% for CAS and smaller than 3% for Q98.

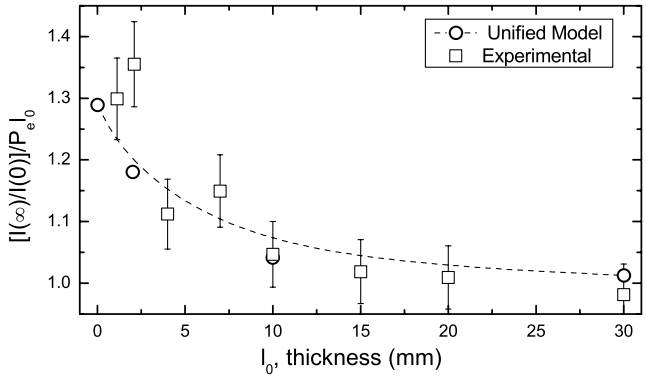

Fig. 4. Normalized TL amplitude, $[I(\infty)/I(0)]/(P_e l_0)$, versus l_0 for BK7. Dashed line is a guide for the eye.

usually positive contributions of the expansion and stress. In this case, the discrepancy between χ^0 and χ^∞ is remarkable ($\chi^0 \simeq 4\chi^\infty$) due to the relative larger contribution of the stress. The averaged thermal diffusivities were found to be $D = (5.0 \pm 0.4) \times 10^{-7}$ m^2 s^{-1} for CAS and $D = (3.0 \pm 0.3) \times 10^{-7}$ m^2 s^{-1} for Q98. These values are within the expected values for these materials [14,15].

Figure 4 shows the amplitude (steady-state signal) of the TL signals normalized by the product $P_e l_0$ as a function of l_0 for BK7 samples with thicknesses varying from 1.1 to 30 mm. The amplitude of the TL signal is very small ($\theta_T \approx 10^{-3}$) due to the very small absorbance at 514.5 nm ($\sim 2 \times 10^{-3}$ cm^{-1}), and consequently the experimental uncertainty is larger than in Fig. 3. Even though, it can be clearly seen that the signal increases as the thickness decreases, in agreement with $\chi^0 \simeq 1.3\chi^\infty$, as expected from calculated published data (Table 1). In this case, the experimental data is compared with transient curves obtained by the unified model (Eq. 5) and is in very good agreement for all thicknesses.

It is important to mention that the simplified and unified theories assume the excitation beam radius, w_{0e}, to be constant inside the sample along the z-direction. This approximation has been tested by comparing numerically the intensity signal using $w_e(z) = w_{0e}$ and $w_e(z) = w_{0e}\sqrt{1 + [(z - l_0/2)/z_c]}$, and it was found that the error between the two is less than 0.5%.

In conclusion, we have performed the first experimental validation, to our knowledge, of the recently proposed model to describe the laser-induced wavefront distortion in optical elements using the TL technique. We showed that consistent values are obtained, irrespective to the sample thickness, when we apply the unified model to describe the laser induced wavefront distortion (TL effect). The results allow us to obtain more accurate physical properties from TL experiments. In addition, for the laser source designers, the unified solution for the optical path in analytic terms, regardless of the thickness of the element, allows the calculation of the TL effect in optical materials without the use of special numerical codes.

The authors are thankful to the Brazilian Agencies CAPES, CNPq, and Fundação Araucária for the financial support of this work.

References

1. W. Koechner and M. Bass, *Solid-State Lasers: A Graduate Text* (Springer, 2003).
2. C. Zhao, J. Degallaix, L. Ju, Y. Fan, D. G. Blair, B. J. J. Slagmolen, M. B. Gray, C. M. Mow Lowry, D. E. McClelland, D. J. Hosken, D. Mudge, A. Brooks, J. Munch, P. J. Veitch, M. A. Barton, and G. Billingsley, Phys. Rev. Lett. **96**, 231101 (2006).
3. W. Winkler, K. Danzmann, A. Rüdiger, and R. Schilling, Phys. Rev. A **44**, 7022 (1991).
4. M. Sparks, J. Appl. Phys. **42**, 5029 (1971).
5. C. A. Klein, Opt. Eng. **29**, 343 (1990).
6. J. Shen, M. L. Baesso, and R. D. Snook, J. Appl. Phys. **75**, 3738 (1994).
7. A. A. Andrade, T. Catunda, I. Bodnar, J. Mura, and M. L. Baesso, Rev. Sci. Instrum. **74**, 877 (2003).
8. L. C. Malacarne, N. G. C. Astrath, and M. L. Baesso, J. Opt. Soc. Am. B **29**, 1772 (2012).
9. L. C. Malacarne, N. G. C. Astrath, and L. S. Herculano, J. Opt. Soc. Am. B **29**, 3355 (2012).
10. http://www.opticsinfobase.org/spotlight.
11. S. M. Lima, J. A. Sampaio, T. Catunda, A. C. Bento, L. C. M. Miranda, and M. L. Baesso, J. Non-Cryst. Solids **273**, 215 (2000).
12. C. Jacinto, A. A. Andrade, T. Catunda, S. M. Lima, and M. L. Baesso, Appl. Phys. Lett. **86**, 034104 (2005).
13. C. Jacinto, T. Catunda, D. Jaque, L. E. Bausá, and J. García-Solé, Opt. Express **16**, 6317 (2008).
14. A. Steimacher, N. G. C. Astrath, A. Novatski, F. Pedrochi, A. C. Bento, M. L. Baesso, and A. N. Medina, J. Non-Cryst. Solids **352**, 3613 (2006).
15. L.-G. Hwa, J. Raman Spectrosc. **29**, 269 (1998).
16. L. C. Malacarne, N. G. C. Astrath, G. V. B. Lukasievicz, E. K. Lenzi, M. L. Baesso, and S. E. Bialkowski, Appl. Spectrosc. **65**, 99 (2011).